Science Advances
AAAS

advances.sciencemag.org/cgi/content/full/6/30/eaba3916/DC1

Supplementary Materials for

Proteasomal degradation of the intrinsically disordered protein tau at single-residue resolution

T. Ukmar-Godec, P. Fang, A. Ibáñez de Opakua, F. Henneberg, A. Godec, K.-T. Pan, M.-S. Cima-Omori, A. Chari, E. Mandelkow, H. Urlaub, M. Zweckstetter*

*Corresponding author. Email: markus.zweckstetter@dzne.de

Published 22 July 2020, *Sci. Adv.* **6**, eaba3916 (2020)
DOI: 10.1126/sciadv.aba3916

This PDF file includes:

Supplementary Materials

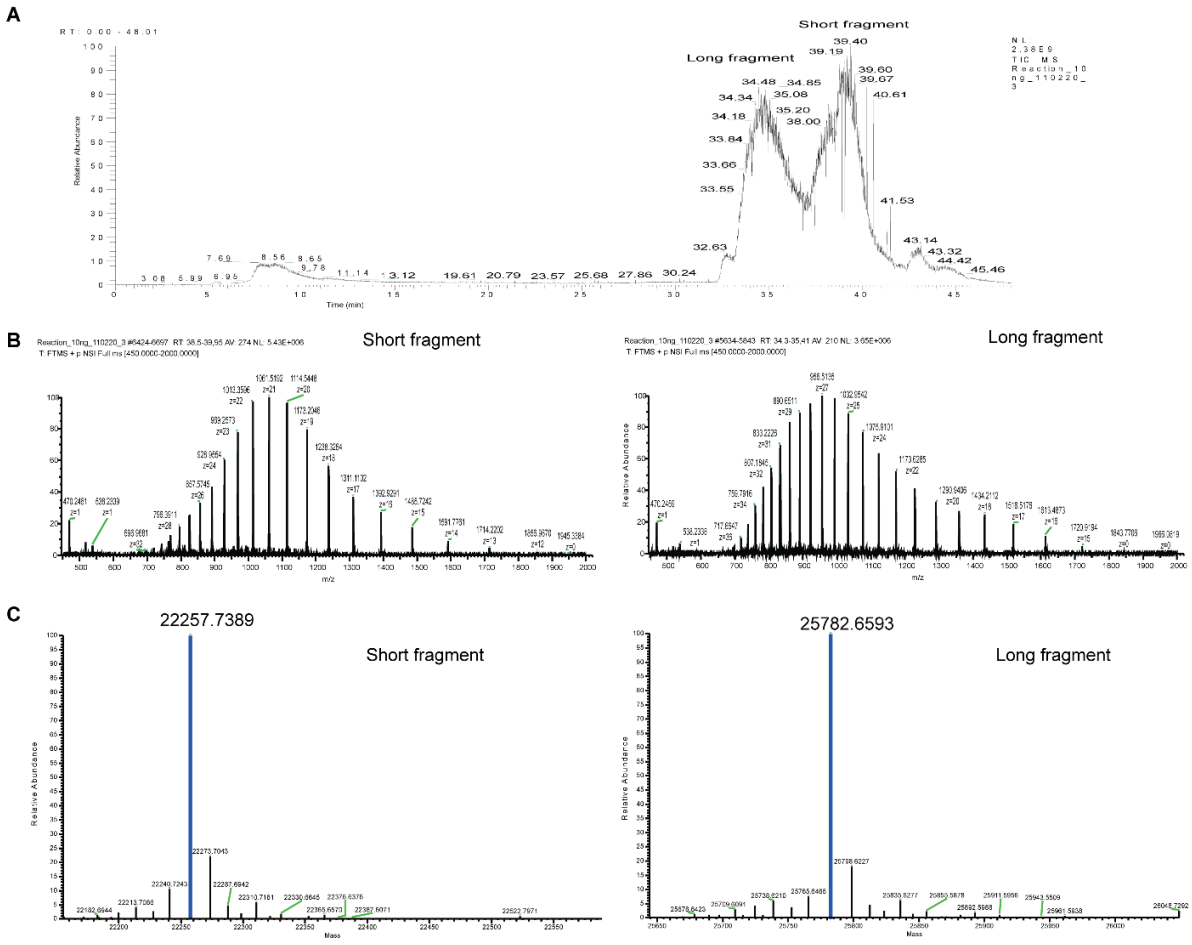

Fig. S1. Analysis of the two long tau fragments using intact MS. (A) Base peak chromatogram displaying well resolved peaks from the two fragments. (B) Original mass spectra of the short and long fragment. (C) Deconvoluted spectra of the short (left) and long (right) fragment. The most abundant protein monoisotopic masses were indicated by blue lines. The other masses (black lines) are protein species with modifications.

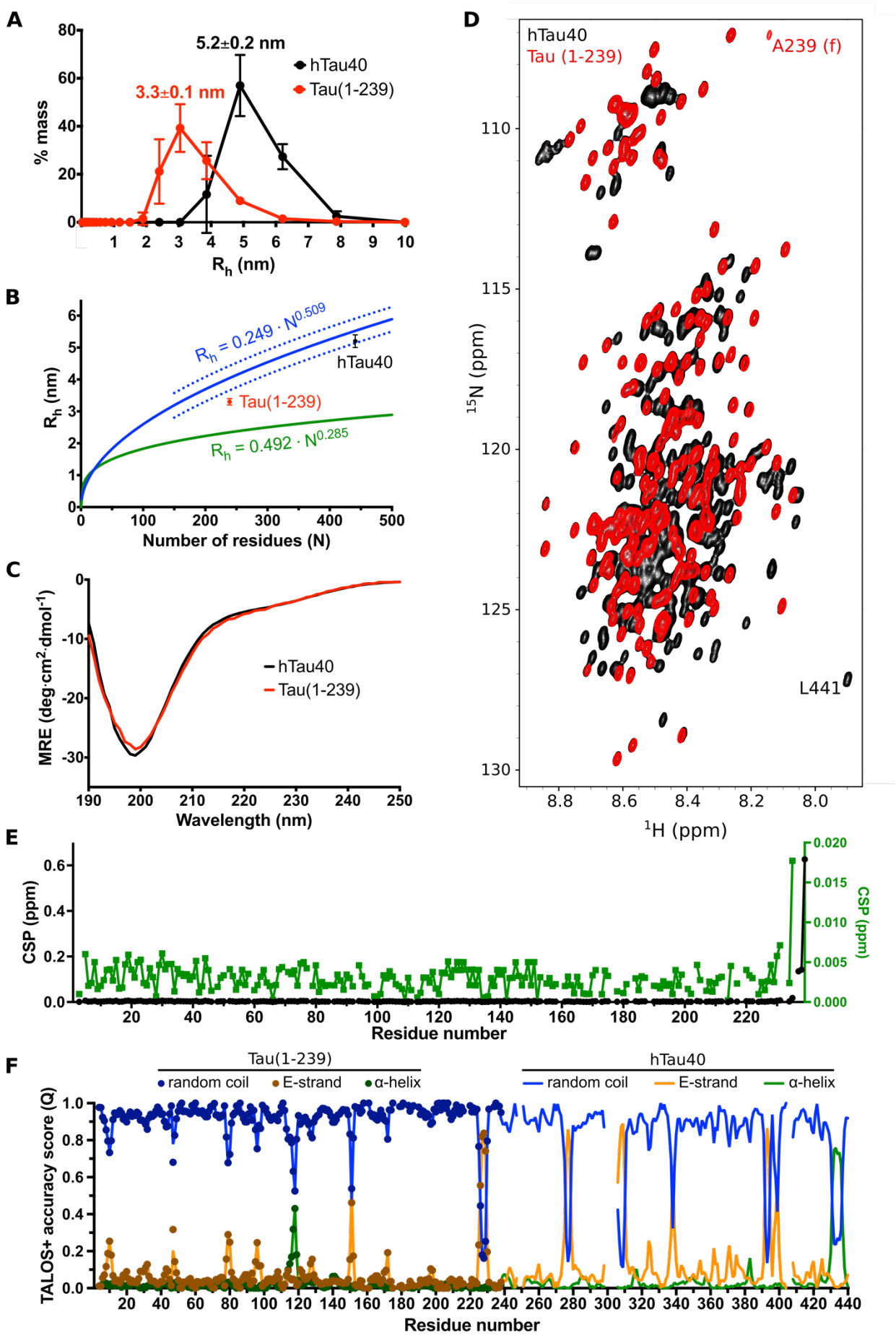
A
5.2±0.2 nm
3.3±0.1 nm
hTau40
Tau(1-239)
% mass
R_h (nm)
B
R_h = 0.249 · N^0.509
R_h = 0.492 · N^0.285
hTau40
Tau(1-239)
R_h (nm)
Number of residues (N)
C
MRE (deg·cm²·dmol⁻¹)
hTau40
Tau(1-239)
Wavelength (nm)
D
hTau40
Tau (1-239)
A239 (f)
L441
¹⁵N (ppm)
¹H (ppm)
E
CSP (ppm)
CSP (ppm)
Residue number
F
Tau(1-239)
random coil
E-strand
α-helix
hTau40
random coil
E-strand
α-helix
TALOS+ accuracy score (Q)
Residue number

Fig. S2. Structural properties of the N-terminal domain of tau. (A) Histogram showing the particle size distribution measured by DLS for hTau40 (black) and Tau(1-239) (red). Error bars represent standard deviation of three independent measurements. Above each graph the average hydrodynamic radius for each protein is shown. (B) Hydrodynamic radius of hTau40 (black) and Tau(1-239) (red) in comparison with the average of experimentally determined sizes for IDPs (blue line) and globular proteins (green line). The equations are attached with the respective text color. For IDPs, which display a greater variation in compaction, the RMSD is plotted as dashed lines. (C) Far-UV circular dichroism spectra of hTau40 (black) and Tau(1-239) (red) plotted as mean residue ellipticity (MRE). (D) Superposition of 2D ^{1}H-^{15}N HSQC spectra of hTau40 (black) and Tau(1-239) (red). The C-terminal residues are labeled, with A239 folded in the ^{15}N dimension. (E) Chemical shift perturbation between hTau40 and Tau(1-239) in full scale (black) and zoomed scale (green). (F) TALOS+ accuracy score (Q) of hTau40 (lines) and Tau(1-239) (dots) for the estimation of α-helix (green/dark green), extended strand (orange/brown) and random coil (blue/dark blue).

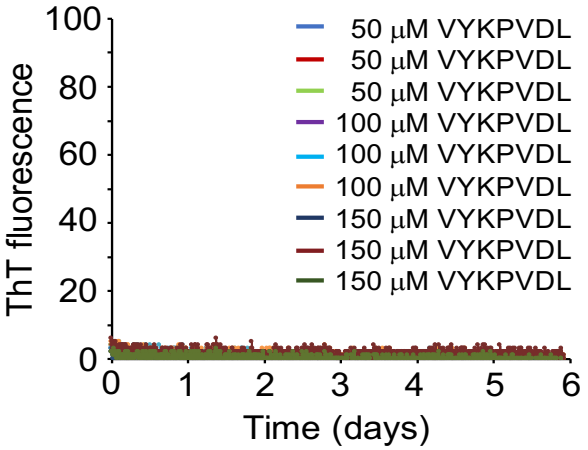

Fig. S3. ThT fluorescence during incubation of the peptide ^{309}VYKPVDL^{315} in the absence of heparin. For each peptide concentration (50 μM, 100 μM and 150 μM), experiments were performed in triplicates.

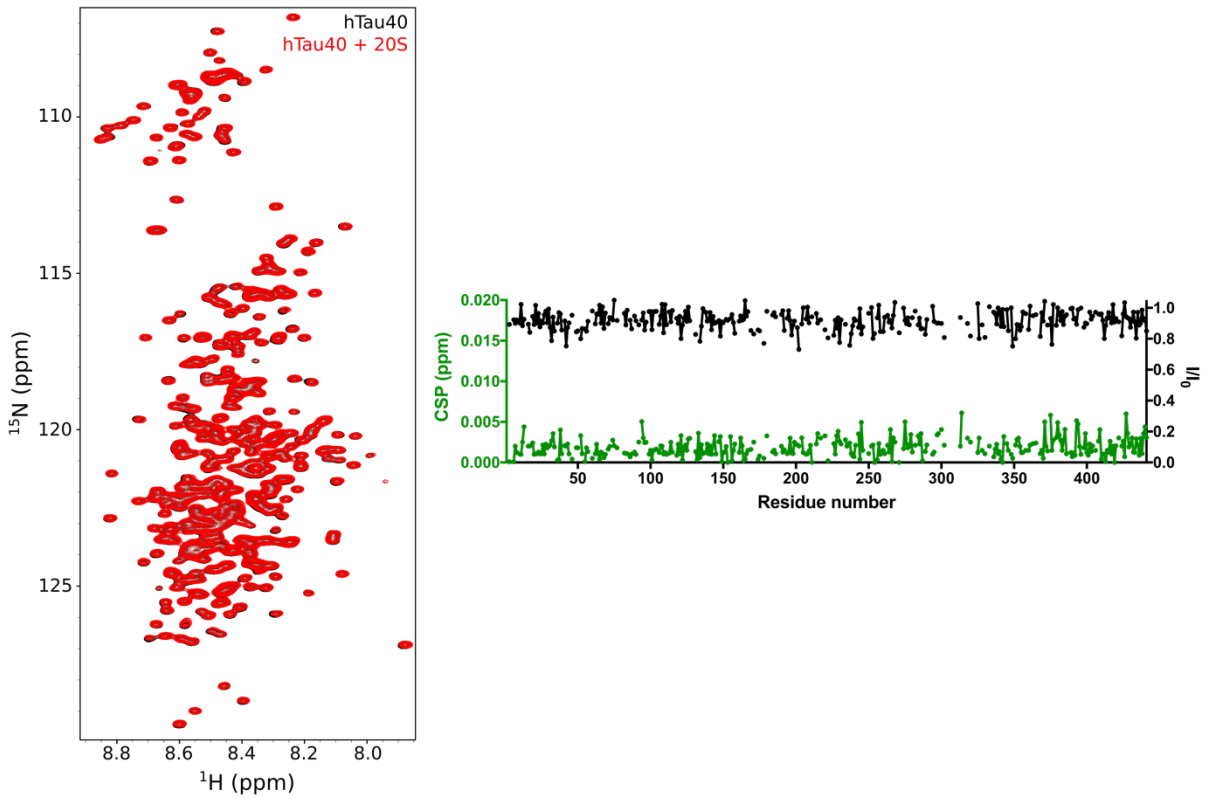

Fig. S4. Analysis of 20S addition on hTau40 spectrum. (left) Superposition of hTau40 ^{1}H-^{15}N HSQC spectrum and hTau40 in presence of the 20S proteasome at 4:1 molar ratio with only 30 minutes of incubation. (right) Chemical shift perturbation (CSP; green) and intensity ratio (black) between hTau40 and hTau40 in presence of 20S proteasome.

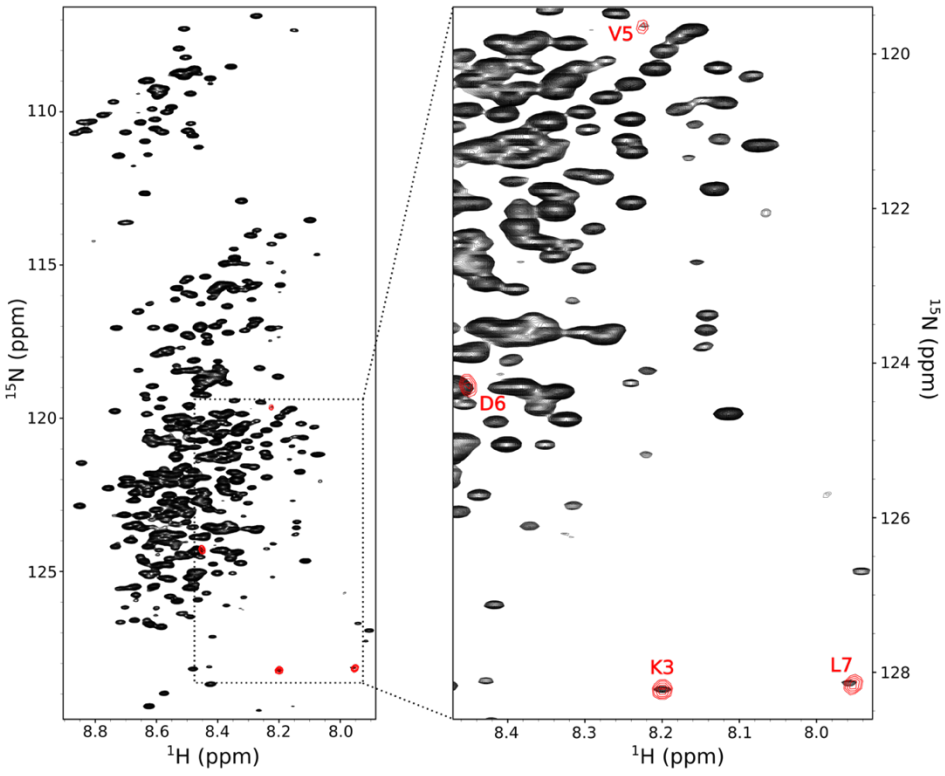

Fig. S5. Superposition of the ^{1}H-^{15}N HSQC of hTau40 at 5 °C in presence of the 20S proteasome after 66 h (black) with a natural abundance ^{1}H-^{15}N HSQC of the ^{309}VYKPVDL^{315} peptide (red), i.e. the peptide with the highest ion peak area in MS. Residue-specific assignment of cross-peaks of the ^{309}VYKPVDL^{315} peptide were obtained by a 2D TOCSY spectrum.

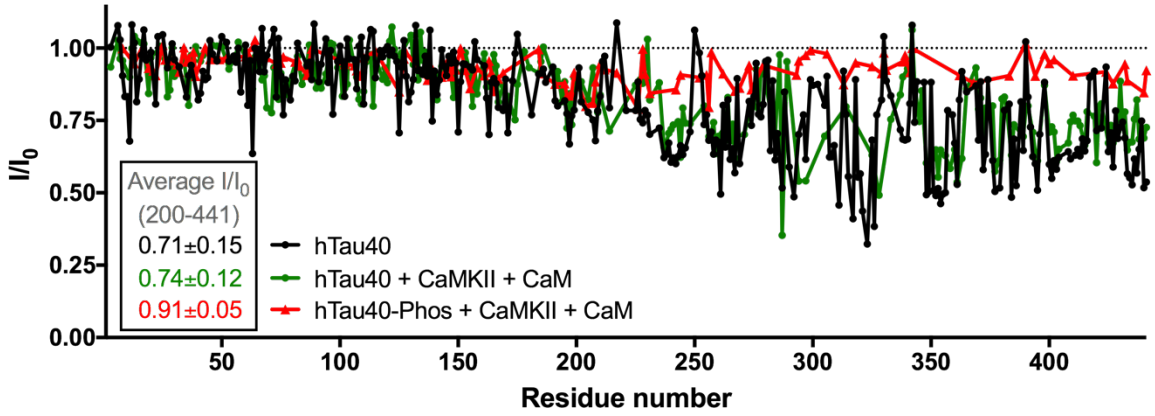

Fig. S6. 20S-degradation of hTau40 in presence of CaMKII and CaM. Final relative peak intensities (after 66 hours) in 2D ^{1}H-^{15}N HSQC spectra are plotted for hTau40 (black), hTau40 in presence of CaMKII and CaM (green) and hTau40 phosphorylated by CaMKII and in presence of CaMKII and CaM (red). The average relative intensities (I/I_0) of the most affected region (200-441) have been calculated. Very similar values were obtained for hTau40 and hTau40 in presence of CaMKII and CaM, while the average relative intensity of phosphorylated hTau40 is substantially larger.

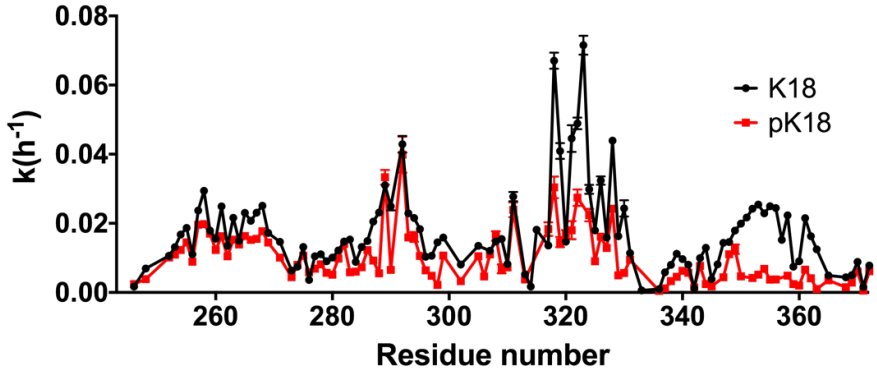

Fig. S7. Residue-specific rate constants of a first-order model of the 20S-degradation kinetics of wild-type (black) and CaMKII-phosphorylated (red) K18 at 5 °C. K18 was phosphorylated at the following sites: S352 and S356 were fully phosphorylated; S324 and S289 were partially phosphorylated (~50%); S262 was only 20-25% phosphorylated. Error bars represent fitting-based std.